Spatial Resolution Enhancement Through Environmental Effects With The Time Reversal Operator Decomposition

PACS numbers: 43.30Gv, 43.30Hw, 43.30Vh

Thomas Folégot[1,2]; Claire Prada[2]; Mathias Fink[2]
1) Atlantide
Technopôle Brest-Iroise, BP 80802
29608 Brest Cedex
France
+33 (0) 298 05.43.21
+33 (0) 298 05 20 34
thomas.folegot@ago.fr

2) Laboratoire Ondes et Acoustique
ESPCI
10, rue Vauquelin
75005 Paris
France
+33 (0) 140.79.44.73
+33 (0) 140 79 44 68
claire.prada-julia@espci.fr; mathias.fink@espci.fr

ABSTRACT

Time Reversal Operator (TRO) Decompositions are performed in a wave-guide using different kinds of bottom. The purchase objective is to study the effects of bottom reverberation and absorption by mean of ultrasonic experiments. Amplitude compensation is proposed to improve the resolution of the system and signal to noise ratio at target. Time dependent reverberation eigenvectors are back propagated in the medium and the conditions of focus on the bottom are discussed.
The results could be used to increase echo levels in shallow water active detection or mine countermeasures.

I. Introduction

Time reversal techniques have been demonstrated in ultrasonics [1] and underwater acoustics environment [2-4]. A derived technique resulting from the analysis of the iterative time reversal process [5] has been developed: the D.O.R.T. method (French acronym for “Décomposition of the Time Reversal Operator”) is a scattering analysis technique using an array of sources and receivers (SRA) [6-7]. This technique shares some of the principles used in eigenvector decomposition techniques for passive source detection [8-9]. However, these last techniques assume statistically uncorrelated sources and require averaging of the measured data, while the time reversal operator decomposition is active and deterministic. It was applied to achieve multi target detection and selective focusing on point like scatterers through inhomogeneous media and in particular in an ideal water wave-guide with a perfectly rigid bottom. Taking advantage of the multiple reflection at the guide interfaces, the method allows large spatial resolution improvement and this super resolution is used to separate the signal coming from close scatterers and then to focus a wave field at anyone of them [10]. This procedure has also been simulated in a Pekeris wave-guide [11, 12]. The method has been used very

recently on simulated reverberation signals [13]. It demonstrated the possibility to increase returned reverberation signal to ambient noise ratio using array beams.
The objective of this paper is to describe the effect on target detection of losses and reverberation in the medium. Thus, from the previous ideal configuration to a realistic model of an ocean wave-guide, three increasingly complex kinds of horizontal bottoms are used in the experiments Fig. 1. The first one is the perfect rigid wave-guide with a steel bottom interface. It induces very low losses, nor reverberation and has a very high critical angle. The second one is a horizontal Plexiglas plate, which induces absorption and has a low critical angle. At last, a steel plate covered with a continuous sandy layer is used, with absorption, a low critical angle and reverberation. The reverberation curve in a monostatic configuration has been measured as shown in Fig. 1. It allows considering this bottom as a realistic reverberating and absorbing medium.

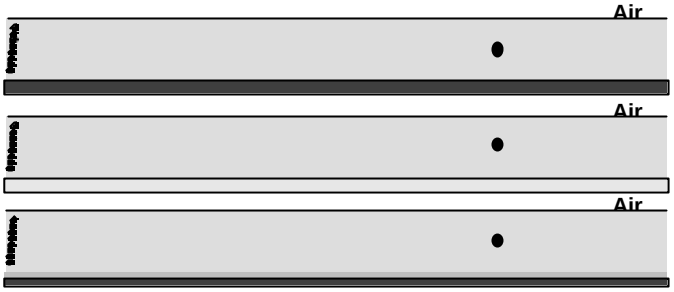

Fig. 1 Three kinds of bottom used for ultrasonic experiments: (a) Perfectly rigid steel bottom, (b) Absorbing Plexiglas bottom and (c) Absorbing and reverberating sand on steel bottom

The D.O.R.T. method is first applied to the detection problem in presence of bottom absorption, which breaks the time reversal invariance. An amplitude compensation technique is proposed in order to restore the time reverse and increase the signal to noise ratio at target while back-propagating the eigenvectors. The benefits of this method, in term of resolution and signal to noise ratio gain, are evaluated using ultrasonic shallow water experiments.
The effect of noise and reverberation is then studied in the model of realistic sandy wave-guide. New eigenvalues appear and are analyzed. After amplitude compensation, the eigenvector is used experimentally for back focus on the bottom. This procedure should be useful to focus energy down inside bottom and increase efficiency of buried targets detection.

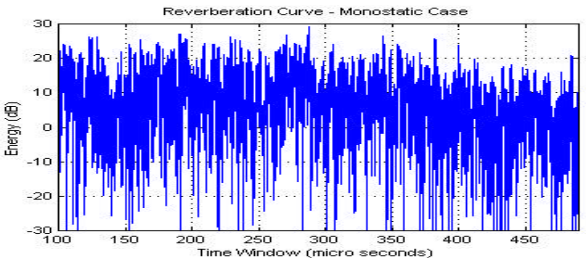

Fig. 2 Monostatic reverberation curve measured for the sand covered steel bottom: the reverberation is due to the sandy layer.

II. Generalized Formulation of Time Reversal Operator Decomposition

The acoustic set consists on a vertical source receiver array of *N* transducers in a time invariant scattering medium. This system is completely described by the inter element response functions $k_{i,j}(t)$ from the element *j* to the element *i*. These inter-element response functions take into account all the environmental effects on the propagation though the medium (reflections, absorption, reverberation and ambient noise) and because of the multiple path propagation, those signals can be relatively long.
Usually, the Time Reversal Operator (TRO) is constructed by the direct measurement of the inter-element impulse functions $k_{i,j}(t)$: a time dependent signal $e(t)$ is emitted successively by each transducer *j* and the jth transducer records :

(EQ I)

$$r_{i,j}(t) = \sum_{j=1,N} k_{i,j}(t) \otimes e(t), \qquad 1 \le j \le N,$$

A more general method consists to emit a family of signals by all the transducers at once, which increase the source level from the number of transducers in the array. Therefore, a Time Reversal Operator can be constructed from the *M* (*M*≥*N*) records along the whole array obtained from a set of M orthogonal emissions. For the m^{th} emission, the *N* receivers signals $r_{i,m}(t)$ can be rewritten through a linear relation :

(EQ II) $$r_{i,m}(t) = \sum_{j=1,N} k_{i,j}(t) \otimes (h_{j,m}.e(t)), \quad 1 \le j \le N,$$

where *e(t)* is the time dependant emitted signal and $h_{j,m}$ the real weighting coefficients that satisfy $\sum_{m=1,M} h_{i,m}.h_{m,j} = \delta_{i,j}$, and $h_{k,l} \in \Re\ (\forall 1 \le k,l \le M)$.

Calling ***K(w)*** the transfer matrix of the system, in the Fourier domain, the previous relation simplifies using matrix formula:

(EQ III) $$R(w) = K(w).H.e(w) = K(w).E_H(w)$$

where $E_H(w)$ and ***R(w)*** are the *NxM* matrices of the Fourier transform of the emitted and recorded signals, and ***H*** the orthogonal matrix $\{h_{j,m}\}_{\substack{j=1,N \\ m=1,M}} \in \Re^N x \Re^M$. If ***H*** is identity, the recorded signals are the widely used signals in the so-called canonical base. If *M=N*, ***R(w)*** is a measure of the transfer matrix in an other basis and the knowledge of ***R(w)*** gives $K(w)=R(w)H(w)^{-1}$. If *M<N*, the emission set is not a basis, but while *M* stays sufficiently larger than the number of targets in the medium, ***R(w)*** provides a good approximation of ***K(w)***.

The time reversal operator was define as $K^{\dagger}(w).K(w)$, where $[]^{\dagger}$ denotes complex conjugate transpose, it is a Hermitian matrix which is diagonalizable in an orthogonal basis [5,6]. Therefore, the time reversal operator $K^{\dagger}(w).K(w)$ is diagonalized at each frequencies. But in practice, it is convenient to calculate the singular value decomposition of the transfer matrix, eventually after matched filtering:

(EQ IV) $$K(w)=U(w)S(w)V^{\dagger}(w).$$

S(w) is a real diagonalized matrix of the singular value decomposition, and ***U(w)*** and ***V(w)*** are unitary matrices. The eigenvalues of the time reversal operator $K^{\dagger}(w).K(w)$ are the squares of the singular values of ***K(w)*** and the eigenvectors are the columns of ***V(w)***. At this stage, we notice that as **H** is a unitary matrix the SVD of ***K(w)*** is simply related to the SVD of ***R(w)***.

The physical meaning of the eigenvalues and eigenvectors of the time reversal operator can be explained as follows. If $T_L(w)$ is the transfer matrix which describes the acoustic propagation between the source receivers array and the scatterers (considered as compression discontinuity only) including all environmental effects; ***C(w)*** is a diagonal matrix of the pointlike targets reflectivities; therefore, the inter elements matrix at frequency w can be written as

(EQ V) $$K(w)=T_L^{*}(w)C(w)T_L(w),$$

where $[]^{*}$ denotes complex conjugate. If T_L is orthogonal, which means that scatterers are well resolved, and according the unicity of the singular value decomposition, *(EQ IV)* provides a SVD and gives the physical meaning of the terms in *(EQ V)*. The number of “non zero” eigenvalues is exactly the number of independent secondary sources given by the resolved scatterers presents in the medium. Time dependent eigenvectors are calculated using a reverse Fourier transform.

III. Effect of Absorption

A. Theoretical approach

Let us consider the general ray-based formulation of the time dependent signal received at hydrophone ***i*** after wave guide multipath propagation of a Dirac emitted by a pointlike source:

$$p_i(t) = \sum_r (L_{r,i}.E).\delta(t - \tau_{r,i}) ,$$

where ***E*** is the maximum amplitude of the source, $L_{r,i}$ is the loss of the r^{th} ray received by hydrophone *i* (0 $L_{r,i}$ 1), and $\tau_{r,i}$ its time delay. The energy of rays is attenuated at each reflection. Thus the higher is the number of reflections, the more attenuated is the ray. Each nonzero temporal eigenvector $V(t) = \{V_i(t)\}_{i=1,N}$ of the Time Reversal Operator has the same multipath structure and can be written with the same convention as:

$$V_i(t) = \sum_r (L_{r,i}.E).\delta(\tau_{r,i} - t)$$

and the pressure at focus location and focus time (*t=0*)

(EQ VI)

$$p_f(t=0) = \sum_{i=1,N} (p_i(t) \otimes V_i(t)) = \sum_{i=1,N} \sum_r L_{r,i}^2 . E$$

The time reversal process is affected by losses in the medium and particularly at the interfaces. Thus the virtual array given by the image theory [1] presents an apodization due to the losses [14]. As a consequence, both vertical and horizontal resolutions are degraded.
In order to strictly compensate this effect, the eigenvector should be transform by multiplying each arrival by $\min(L_{r,i}) / L_{r,i}^2$. This transform provides a uniform amplitude front at focus, and as a consequence, the best time compression and the lowest side lobes. The pressure at focus is

(EQ VII)

$$p_f(t=0) = \sum_{i=1,N} (p_i(t) \otimes V_i(t)) = \sum_{i=1,N} \sum_r \min(L_{r,i}) . E \, .$$

But the signal to noise ratio at focus will be very low because of the addition of the environmental losses. The best way to maximize $\boldsymbol{p_f}$ in order to obtain the best signal to noise ratio at the target location consists in setting the amplitude of each arrival to $\boldsymbol{E}$ by multiplying each arrival amplitude by $1/L_{r,i}$. One effect is to minimize virtual array apodization. In this case, despite higher side lobes the pressure at focus, which writes

(EQ VIII)

$$p_f(t=0) = \sum_i (p_i \otimes e_i) = \sum_i p_i \otimes \sum_r E\boldsymbol{d}(\boldsymbol{t}_{r,i} - t) = \sum_i \sum_r L_{r,i} E \, ,$$

is maximized. The expected gain is in close relation with both the number of array elements and the number of arrivals. In the following sections, we show experimentally the impact of this last weighting technique in comparison with the formally used time reversal operator eigenvectors.

B. Experimental results

The experimental results presented in this paper are made in water tank in the ultrasonic domain. The 40-transducers vertical array has a central frequency of 1.5 MHz and the array pitch is equal to 0.58mm. The water depth is 27mm. A single target (a wire of diameter 0.04λ) is placed in the water column at 330mm range and 20mm above the bottom. The diffraction theory gives for *F>>D* a vertical and horizontal resolution as

$$\Re_z \approx \boldsymbol{l} \frac{F}{D} \text{ and } \Re_x \approx 7\boldsymbol{l} \frac{F^2}{D^2}$$

where $\boldsymbol{l}$ is the wavelength, *F* the range and *D* the array aperture. The acoustic configuration in this experiment gives a theoretical vertical resolution in free space of $14\boldsymbol{l}$ (half of the water depth).
Three different kinds of bottom are used: in Fig. 3, Fig. 4 and Fig. 5 the lower limit is a water/steel plane interface. The critical angle is very high and the losses of reflected rays are due to scattering and diffraction. In Fig. 6, Fig. 7 and Fig. 8, the bottom is made as Plexiglas. Only a few bottom-reflected rays are above electronic noise due to a low critical angle and absorption. At last, a sandy layer is spread above a steel plate to model absorption and bottom reverberation (Fig. 9 to Fig. 11).

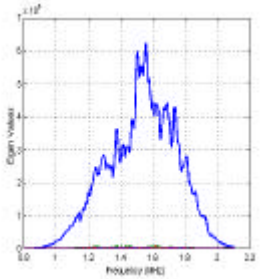

Fig. 3 Experimental evolution of time reversal operator eigenvalues in a rigid waveguide. The frequency band is 0.8MHz to 2.2 MHz.

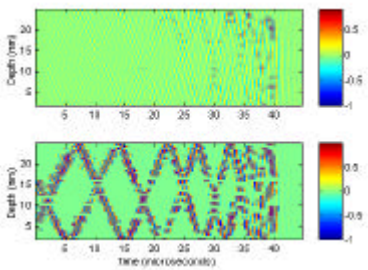

Fig. 4 Normalized time and depth dependent first eigenvector obtained in a perfect rigid wave-guide (up) and after amplitude compensation (down).

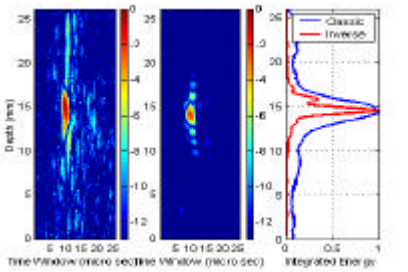

Fig. 5 Focus in a perfect rigid wave guide: the depth and time dependent signals obtained in dB by propagating the eigenvector (left) and the compensated eigenvector (center). The integrated energy versus depth on the right hand shows the gain of the vertical resolution when amplitude is compensated (red curve).

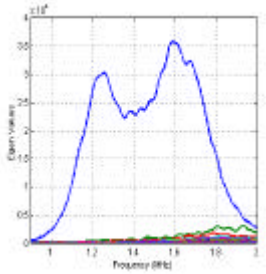

Fig. 6 Experimental frequency dependent TRO eigenvalues in an high level absorbing waveguide made with Plexiglas.

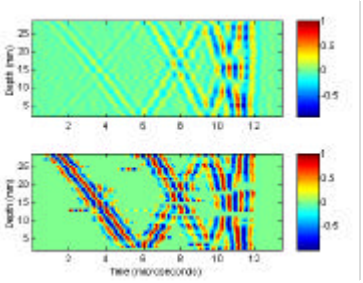

Fig. 7 Normalized time and depth dependent first eigenvector obtained in a wave-guide with bottom absorption (up) and after amplitude compensation (down).

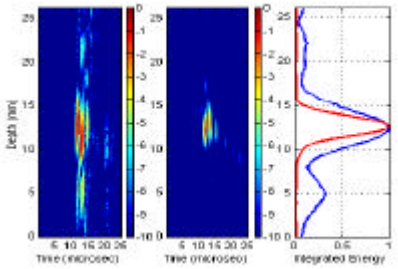

Fig. 8 Effect of amplitude compensation on the focus in an absorbing wave-guide: the depth and time dependent signals obtained in dB by propagating the eigenvector (left), and the compensated eigenvector (center). The integrated energy versus depth on the right hand shows the gain on the vertical resolution when the amplitude is compensated (red curve).

In all cases, the first nonzero eigenvalue corresponds to the single target in the water column. Indeed, the time domain eigenvector obtained by inverse Fourier transform shown for each kind of bottom in Fig. 4, Fig. 7 and Fig. 10 presents series of resolved arrivals and one late unresolved arrival resulting from the interference between the direct rays and the lowest surface bottom reflected rays. The time dispersion of the eigenvectors depends on the absorption as well as the number of resolved arrivals.

Experimentally, in the first kind of bottom the high critical angle of steel allows a large number of attenuated arrivals. Attenuation is due to scattering on the surface and the bottom at each reflection. Therefore, the back propagation of this eigenvector gives a pressure profile focusing at target depth and range. The observed vertical resolution at focus while propagating the first eigenvector without any amplitude compensation is about 4λ (blue curve on the right hand of Fig. 5). Therefore, in this case, the gain using the D.O.R.T. method without amplitude compensation is about *3.5* and the equivalent array aperture in this wave-guide (including apodization) is about *3.5D*. Thus the gain in terms of horizontal resolution is about *12*.

Amplitude compensation of the first eigenvector is performed with the objective to increase as much as possible the acoustic pressure on the target (EQ VIII). As expected, the signal to noise ratio gain is considerable, about *23dB* above the previous case. The vertical resolution is approaching the diffraction limit value of $\lambda/2$ (red curve in Fig. 5). Therefore, the equivalent array aperture is now set to 20 times the instrumental array aperture. The benefit on the horizontal resolution is even more significant: it increase 400 times but the horizontal focus length is also limited by the diffraction limit as shown in 0 (left and center).

In the case of a high absorption level, as observed on the two last bottoms, the high benefit of each amplitude compensation should be in balance with the low number of rays above noise. The number of resolved rays is very limited in the case of absorption bottom but the resolution in both directions remains high (Fig. 8) because of the gain of energy by compensation. The signal to noise ratio at target increases by about *9* to *12dB* by performing the amplitude compensation.

IV. Ambient Noise and Reverberation

Let us consider a single pointlike target in shallow water environment in presence of electronic noise and bottom reverberation. The bottom is a steel base covered by a sandy layer that creates a realistic model of bottom reverberation.

A. Ambient Noise

Below the first singular value, the non-zero noise singular values are the signature of electronic, ambient and reverberation noise. Electronic and ambient noises are independent of the source level or the emission basis used for the inter-elements matrix acquisition. As a

consequence, the ambient noise singular values levels do not depends on source level or emission basis and target eigenvalue improve with average increase of emitted energy. The detection threshold should be improved in the same proportions.

B. Reverberation

Lingevitch et al. [13] extended theoretically the focus with a time reversal operator to the case of stochastic reverberation returns from a rough sediment interface in an ocean waveguide. He demonstrated numerically that the returned signal focus at the rough bottom interface. Here, the Time Reversal Operator is constructed in presence of a single pointlike scatter at depth 8.5mm and range 330mm in a 25mm high wave-guide. Fig. 9 shows the eigenvalues versus frequency in each case. Non-zeros eigenvalues appear in these curves. In order to understand the physical meaning of this additional eigenvalues, two different orthogonal emission sets are used: the canonical basis and the Walsh basis. The singular values are *N* times higher for the Walsh codes than for the canonical emission (*N* being the number of array elements). However, at each frequency, the relative levels of the singular values are unchanged.

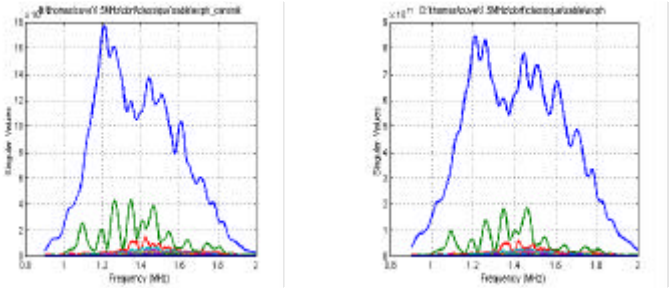

Fig. 9 Experimental frequency dependant TRO eigenvalues in a realistic ocean wave-guide with absorption and reverberation.

The two first eigenvectors are calculated and back propagated using *H=I*. The corresponding pressure fields around the target position shows spatial and temporal focusing at target depth and range for the first eigenvector, while the focusing is achieved on the sandy floor at the same range for the second eigenvector. These results confirm two major properties of the D.O.R.T. method: first, the capability to take advantage of the environment, multipath propagation and use returned reverberation signals for increase signal to noise ratio on localized areas. Second, as a kind of consequence, the capability for selective focusing between reverberation and target.

This result is non-trivial because of the spatial dispersion of the bottom speckle and the spatial focus zone is highly dependent of the time window length used in the Time Reversal Operator. In fact, for increasing resolution the method needs to take into account all the time dispersion of echoes. But this time window have to be limited because the continuity of the targets distribution in the bottom. In the experiment presented in Fig. 10 and Fig. 11, the time window is 25µs, which allows about 8 or 9 reflected rays as shown by the first time dependent eigenvector associated to the pointlike target (left hand of Fig. 10). The ranges of focus for both eigenvectors are the same and the focus sizes are both of same order. Because the time window at acquisition starts at the first arrival, the spatial distribution of targets is located at the beginning of the spatial area defined by the acquisition length. This can be explained by the decreasing of the global reflection index with range due to propagation losses. The D.O.R.T. method makes spatial selection also on the bottom, and allows focusing on its most reflective part. The characteristic size of focus on the bottom is given by the resolution of the complete system, composed by array configuration, ocean environment and post processing treatment like amplitude compensation.

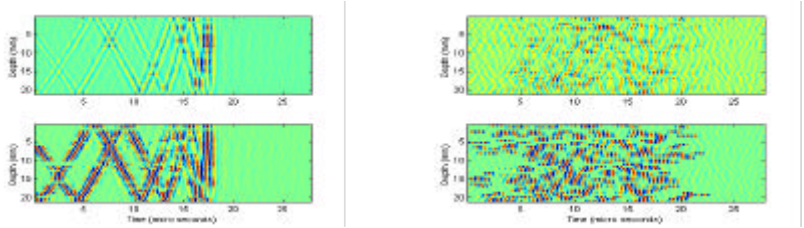

Fig. 10 First (left) and second (right) normalized eigenvectors obtained in the realistic ocean wave-guide (up) and after amplitude compensation (down).

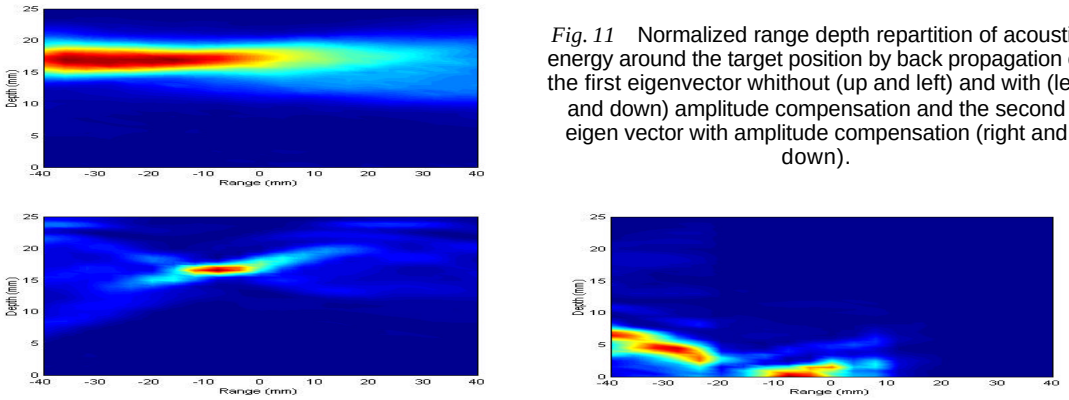

Fig. 11 Normalized range depth repartition of acoustic energy around the target position by back propagation of the first eigenvector whithout (up and left) and with (left and down) amplitude compensation and the second eigen vector with amplitude compensation (right and down).

V. Conclusion

This study leads to application in underwater warfare and mine countermeasure. It shows the huge benefits of amplitude compensation for increasing the signal to noise ratio at target and the vertical and horizontal resolution. The signal to noise ratio gain and the size of focus is directly connected to the array configuration, the environment characteristics and the art of amplitude compensation. Array configuration defines the basic resolution, the range limits of detection and the quality of focus by setting the level of side lobes. Environment and amplitude compensation gives the gain of vertical and horizontal resolution and defines possibilities for focusing on the bottom or eventually on the sea surface. These results should be useful for targets in the water column in noisy environments such as shallow water oceans, and also for objects buried in sediment.

VI. References

[1.] P. Roux, B. Roman, M. Fink, "*Time-reversal in an ultrasonic waveguide*", Appl. Phys. Lett.,**70** (14), 1811-1813, April 1997.
[2.] D.R. Jackson and D.R. Dowling, "*Phase conjugation in underwater acoustics*", J.Acoust.Soc.Am., **89** (1), 171-181, (1991).
[3.] W.A. Kuperman, , T. Akal, C. Ferla, and D. R. Jackson,, "*Phase conjugation in the ocean: Experimental demonstration of an acoustic time-reversal mirror*", J. Acoust. Soc. Am., **103** (1), 25-40, (1998).
[4.] W.S. Hodgkiss, H.C. Song, W.A.Kuperman, T. Akal"A, C. Ferla, D.R. Jackson, "*Long-range and variable focus phase conjugation experiment in shallow water.*" J. Acoust. Soc. Am., **105** (3), 1597-1604, (1999).
[5.] C. Prada, J.L Thomas, M. Fink, "*The iterative time reversal process :analysis of the convergence*", J. Acoust. Soc. Am., **97** (1), 62-71, (1995).
[6.] C. Prada, M. Fink, *Eigenmodes of the time reversal operator: a solution to selective focusing in multiple target media*", Wave Motion, Vol 20, 151-163, (1994).
[7.] C. Prada, S. Manneville, D. Spoliansky, M. Fink, "*Decomposition of the time reversal operator : detection and selective focusing on two scatterers*"
[8.] G. Bienvenu and L. Kopp, "*Optimality of high resolution array processing using the eigensystem approach*," IEEE Trans. Acoust. Speech and Sig. Proc. **31** (5) (1983).
[9.] Ralph O. Schmidt, "*Multiple Emitter Location and Signal Parameter Estimation*,"
IEEE Trans. Ant. and Prop., **AP-34** (3) 276-281 (1986).
[10.] N. Mordant, C. Prada and M. Fink*, "Highly resolved detection and selective focusing in a waveguide using the D.O.R.T. method"*, J.Acoust.Soc.Am. 105, 2634-2642 (1999).
[11.] C. Prada, T. Folégot, N. Mordant, and M. Fink*, "Time Reversal Operator Decomposition in a Ocean Wave Guide*", Proceedings of the 5th Underwater Acoustics Journeys, Brest, France, 2000.
[12.] T. Yokoyama, T. Kikuchi, T. Tsuchiya and A. Hasegawa*, "Detection and selective focusing on scattering using decomposition of Time Reversal Operator Method in Pekeris Waveguide Model"*, Jap. J. Appl. Phys., **40**, 2001
[13.] J.F. Lingevitch, H.C. Song and W.A. Kuperman, «Time reversed reverberation focusing in a waveguide », *J. Acous. Soc. Am.*, submitted January 20, 2001.